JPL D-1183

SP-100 PROGRAM

Technical Information Report

SP-100 System Definition Conceptual Reference Design Activities: February Through June 1983

James W. Fortenberry
Donald M. Moore
S. Walter Petrick
Richard H. Smoak

December 1983

National Aeronautics and
Space Administration

JPL

Jet Propulsion Laboratory
California Institute of Technology
Pasadena, California

DISCLAIMER

JPL D-1183

SP-100 PROGRAM

Technical Information Report

SP-100 System Definition Conceptual Reference Design Activities: February Through June 1983

James W. Fortenberry
Donald M. Moore
S. Walter Petrick
Richard H. Smoak

December 1983

DISCLAIMER

National Aeronautics and
Space Administration

JPL

Jet Propulsion Laboratory
California Institute of Technology
Pasadena, California

SP-100 PROGRAM

Department of Defense
Defense Advanced Research Projects Agency
Arlington, Virginia

Department of Energy
Office of Nuclear Energy
Washington, D.C.

National Aeronautics and Space Administration
Office of Aeronautics and Space Technology
Washington, D.C.

Jet Propulsion Laboratory
California Institute of Technology
Pasadena, California

ABSTRACT

The original SP-100 conceptual system design was examined from the mechanical design and integration viewpoint for the purpose of updating the design, identifying concerns, and providing recommendations for future work. Some of the findings were that: integration of heat pipes into the radiator structure appears practical, but a number of problems remain to be addressed and resolved through development effort; thermal and structural interfacing of the shield and defining shield weight are key areas that need to be addressed; the radiator may be critical in shell buckling which would make beryllium a leading candidate material; material problems such as beryllium vs. shuttle fracture mechanics criteria need to be addressed.

CONTENTS

FIGURES | Page

TABLES

Section 1

Introduction

The System Definition Team members examined the original SP-100 Conceptual Design from the mechanical design and integration viewpoint for the purpose of providing an updated or reference design. To provide this perspective, the support of thermal control, structures, and materials disciplines was required.

This report is presented in four sections. Section 2 summarizes the reviews of activities in the format of the concerns and the recommendations for future work. Section 3 outlines the reference SP-100 design and presents the requirements and configuration upon which the discipline comments are based.

Finally, the discipline support summaries are compiled in Section 4 for future reference. The reader is encouraged to review these for more detailed information and recommendations concerning the SP-100 Reference Design.

Section 2

Summary and Recommendations

During the course of Design Team activities, technology areas that require further investigation have been identified. The conceptual design work that led to these recommendations is contained within the body of this report, but an attempt has been made to summarize these findings in this Section.

An SP-100 system mass of about 3600 kg was estimated. The zone of greatest uncertainty is the radiation shield which comprises 38% of the mass. The shield and conversion subsystems combined account for 75% of the SP-100 mass estimate. Beryllium has been identified as a leading candidate material for the radiator structure because of its high specific stiffness.

The SP-100 reference design was partitioned into five thermal control zones for the purpose of identifying technology requirements: (1) reactor, (2) heat pipes, (3) radiation shield, (4) radiator, and (5) power processing/control electronics.

2.1 Reactor

No conceptual design activity occurred in this area other than examination of the thermal integration of the reactor into the overall system. Suggested future activity in this area includes establishing interfaces with adjacent thermal zones, the design of a multilayer insulation system, development of structural design concepts, and materials compatibility. The materials problems appear formidable enough to suggest an accelerated test program as a high priority consideration.

2.2 Heat Pipes

Integration of the heat pipes within the radiator structure appears practical, but the transition area from the reactor through the radiation shield to the radiator poses problems. The multiple bends required could adversely affect heat pipe performance. The reference configuration is new and untried, and analysis and testing are strongly recommended to determine if the heat pipes can be fabricated to the SP-100 configuration and still meet the performance requirements. Definition of interface requirements and the start-up and shut-down dynamics is another area of recommended investigation. The materials compatibility of the working fluid wick structure, and container should also be examined.

2.3 Radiation Shield

The shield design consists only in the form of a simplified geometrical concept. Much work remains to be done in this, the heaviest of all SP-100 subsystems. A recommended future activity in this thermal zone includes the structural design and integration of the shield and the other components that interface with it. This would include defining the structural/thermal interfaces with the other zones and design of the multilayer insulation blanket. Considerable analytical modeling will be required to refine the temperature limits and prepare conceptual absolute temperature control designs, and to utilize concepts such as active thermal control.

2.4 Radiator

Selection criteria for the proposed radiator material were specific stiffness and specific strength over the temperature range of 300^{o}-950^{o}K. Studies have indicated that the radiator may be critical in shell buckling, which made beryllium the leading candidate material.

The 20^{o} conical radiator concept lends itself to modular design with thirty-two equal area panels sized to generate electrical power in equal voltage increments of approximately 200 V. The panel lengths and heat pipe support requirements appear to be roughly compatible which should permit assembly integration. Considerable investigation remains for the radiator including: additional work on the individual panels' joint design; the effects of loads caused by free flight maneuvers, thermal shock/transients, and shuttle cradle interfacing; the possibility of radiator shapes other than conical as well as deployable concepts; material problems such as beryllium vs. shuttle fracture mechanics criteria or the lack of a long term, high temperature, high emittance outer coating.

2.5 Power Processing/Control Electronics

The extended radiator concept, devised to provide a low-temperature thermal zone for the electronics, adds undesired length to the overall SP-100 configuration. Future investigation in this area should include concepts for minimizing length and more detailed interface and requirements definition.

Section 3

Reference Design

The original basis for the design was Reference 1. During the course of Team activities, it was decided that the reference design would be based on a modified 20° half-cone angle concept in Reference 2. The main differences between the original and current designs was the thermoelectric conversion system which was modified to reflect radiator area limitations and revised performance parameters. These differences are summarized in Table 3.1.

The resources did not permit an overall, comprehensive analysis of the configuration. Since the heart of the original SP-100 concept was the thermoelectric conversion subsystem, the team decided to investigate the radiator and heat pipe feasibility first. This was accompanied by the identification of thermal zones (or interfaces) from which design concepts and technology concerns could be derived. This led to the mechanical/thermal design concepts and mass estimate described herein.

3.1 Radiator/Heat Pipes

The radiator/heat pipes are treated as an integral assembly because of the considerations outlined in Figure 3-1.

Table 3-1

Comparison of Thermo Electric Power Conversion Systems

System	Power (KWe)	Eff. %	Radiator Area (M)	Cone Half Angle	Temp K Hot Shoe	Temp K Cold Shoe
Original (Ref 1)	100.0	6.8	69.12	15^{o}	1355	840
Reference Design (Ref 2)	82.6	6.4	48.71*	20^{o}	1380	932

*Update area based on characteristic length.

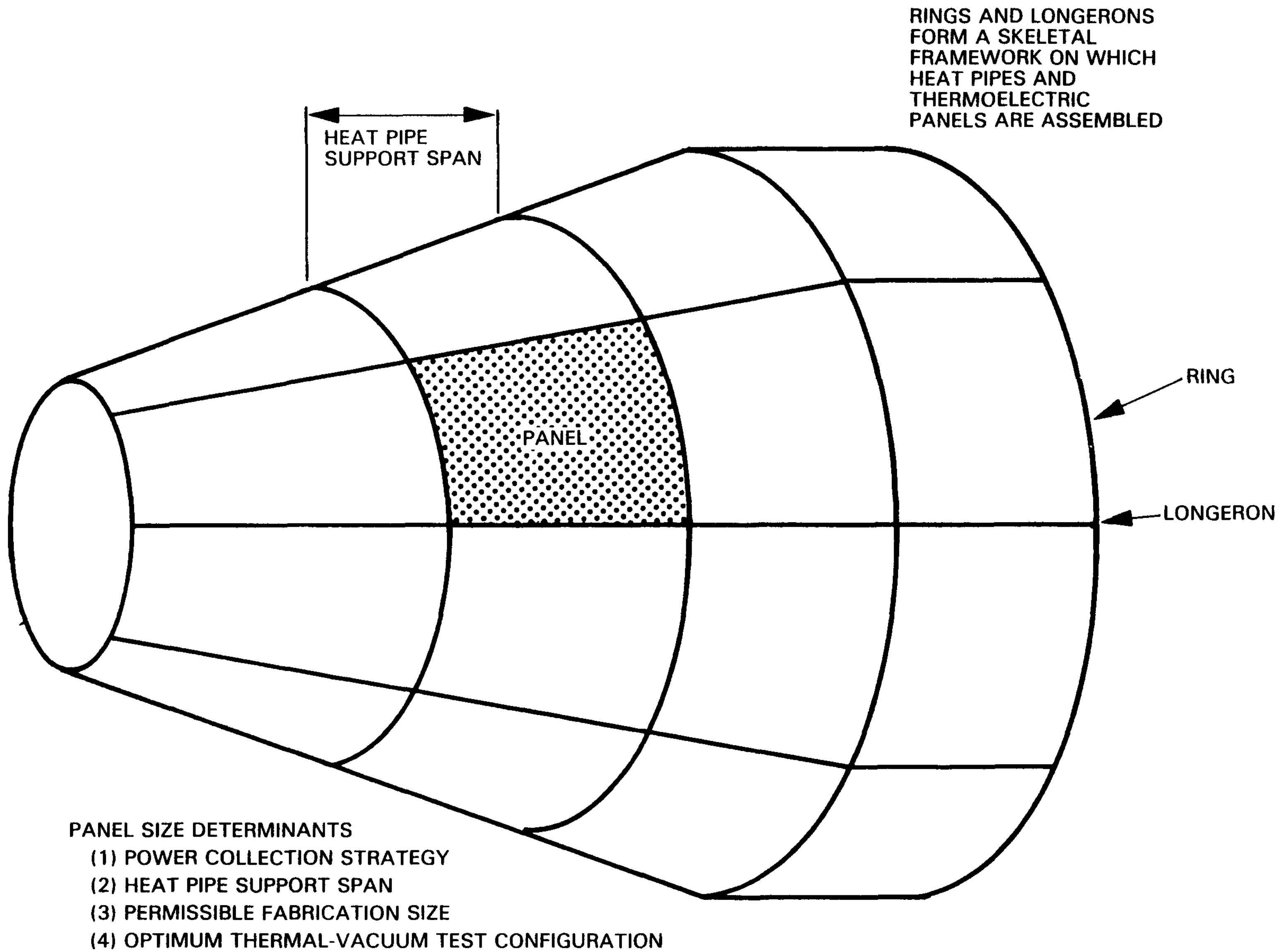

Figure 3.1 Thermoelectric Power Plant Support Framework Concept

The primary design driver for the conical radiator shown turned out to be the panel size which was influenced by heat pipe support span, permissible fabrication size, optimum thermal vacuum test configuration, and power collection strategy.

The heat pipe support span requirements were analyzed by assuming the heat pipes as simply supported beams within an assumed supporting framework. With this assumption, two conditions would determine the support span: deflection and/or bending stress due to dynamic loading during launch. Assuming the heat pipes can be located at a radial clearance of 6-20 cm (2.36-7.87 in) from the hot shoe of the panel, it does not appear that heat pipe impingement on the hot shoe due to dynamic deflection is the major factor. It appears that the limiting factor on heat pipe support would be bending stress on the pipes. Since the strength properties of the heat pipes are unknown, this conclusion will have to be re-examined should this configuration be pursued further. Subject to the bending strength of the heat pipes, unsupported lengths of 0.9 - 1.5 M (36-60 in) may be practical but intuition supports the lower (36-in) limit.

The permissible fabrication size and an optimum thermal-vacuum test configuration are closely tied-in with the power collection strategy of the thermoelectric/radiator panels which turned out to be the deciding factor in the overall radiator configuration. In order to collect the power in equal voltage increments of approximately 200v, the thermoelectric/radiator assembly was divided into 32 equal areas as shown in Figure 3.2. This will require further study since it will be noted from Figure 3.2 that the longest panel lengths (which determine the support frame distance and, hence, the unsupported heat pipe span) would be 1.614-M (63.50-in) which is probable at or exceeds the limit of heat pipe bending strength capability. This is recommended as a subject for future investigation.

The preceding arguments have led to the support assembly concept shown in Figure 3.2 and described in Section 4.1. The division of the radiator into 32 equal areas dictates an arrangement of support frames or rings necessary to provide lateral or hoop stiffness and support, particularly at the forward and aft support points. Longitudinal/meridional support would be provided by the shell itself in the form of its basic membrane thickness. The basic single panel structure described in Section 4.1 would have outward facing flanges on all four sides which, when bolted together, would provide considerable hoop and longitudinal stiffness. The assembly sequence would start with the placement of each heat pipe on a skeletal framework which could be integrated into the radiator panel joints. The heat pipe supports at each ring would provide for only radial restraint which would allow the heat pipes freedom to expand axially.

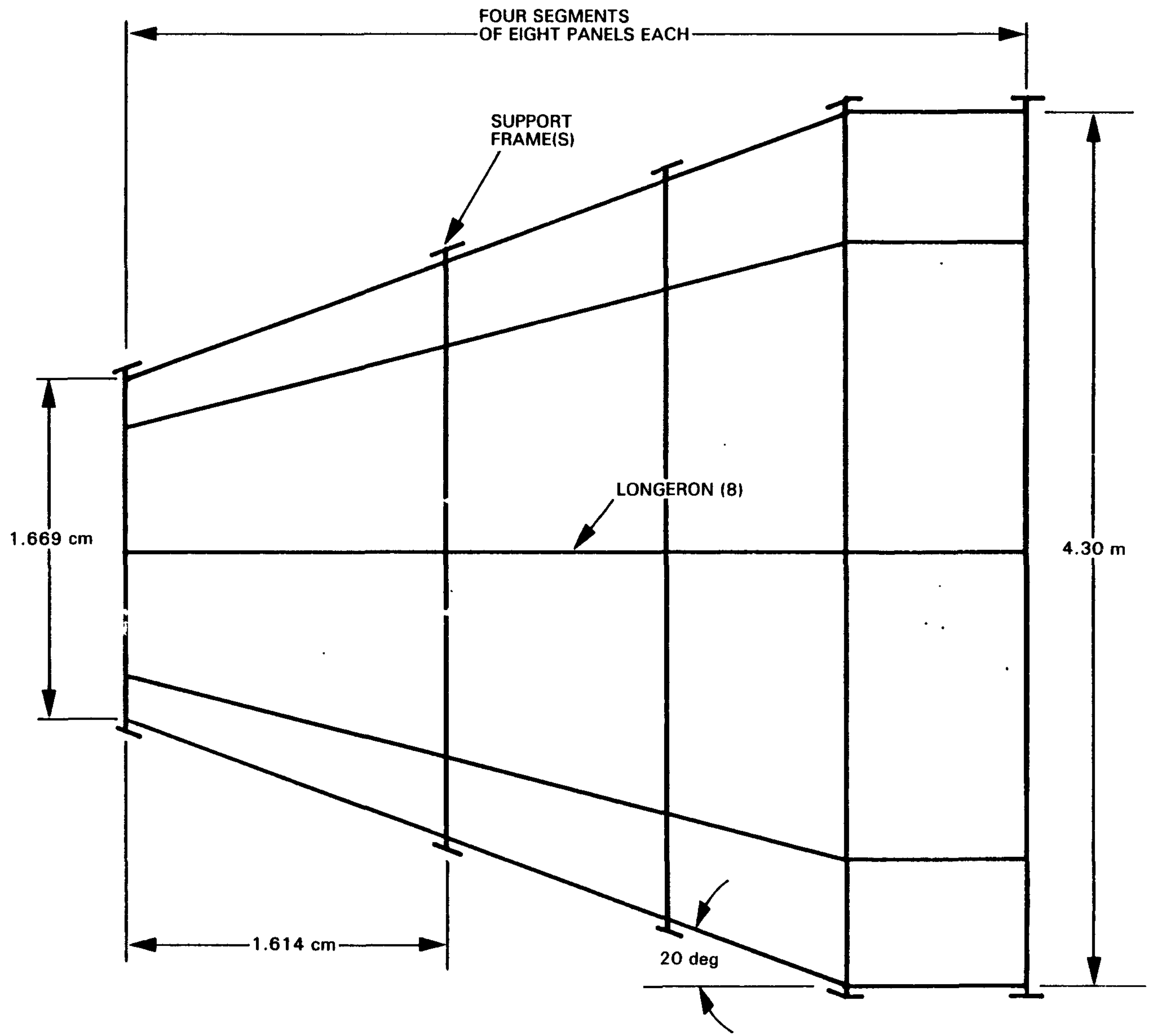

Figure 3.2 Thermoelectric Power Plant Envelope and Radiator Configuration (32 Equal Area/Voltage Panels)

The installation of 120 continuous heat pipes within the radiator framework appears to be straightforward and practical - achievable through good design practice. However, the heat pipe transition area from the reactor through the shield to the radiator presents some special problems. Regardless of whether the heat pipes are routed directly through the shield or around the shield, multiple bends of the heat pipes would be required as shown in Figures 3.3 and 3.4. The routing shown (around the shield) would gather up the 120 heat pipes and divide the group into four quadrants of tightly merged bundles of 30 heat pipes each through a series of multiple bends of the heat pipes. Each bundle would then be routed through a channel notched on the shield's external surface. After traversing the length of the shield, the heat pipe bundles, through another series of multiple bends would disperse about the radiator skeletal framework. It appears that distances/gaps between the reactor/shield and shield/radiator would be adequate to satisfy the multiple bend requirements if MIL-STD values of tube bend radii can be used. However, the ability of heat pipes' internal workings and components to withstand such bending is unknown and will have to be investigated.

3.2 Thermal Control Zones

In order to establish the anticipated thermal environment for SP-100 components, preliminary thermal control zones and interfaces were established (Figure 3.5) using the assumptions noted in Table 3.2. These zones, in forward to aft order, are: reactor, heat pipes, radiation shield, radiator, and the power processing/control electronics. The team activity evolved no specific reactor design concepts but places its main concern with thermally integrating the reactor into the overall thermal system.

The present conceptual thermal design assumes that the reactor is covered with a high temperature, multilayer insulation (MLI) blanket. Heat transfer to other zones, other than by the heat pipes, is minimized by the use of MLI to attenuate the radiation heat transfer and by the use of thin wall titanium tubing for mechanical supports to attenuate the conductive heat transfer. As shown in Section 4.2, the reactor must generate about 2000 kw to supply 1,600 kw to the power system while the remaining 400 kw is lost through the MLI to space.

A primary concern of this thermal configuration, which depends on heat pipes for the heat transport from reactor to thermoelectric converter is heat pipe start-up. Successful heat pipe start-up will depend upon, as a minimum, the length of the heat pipe, amount of heat being transferred,

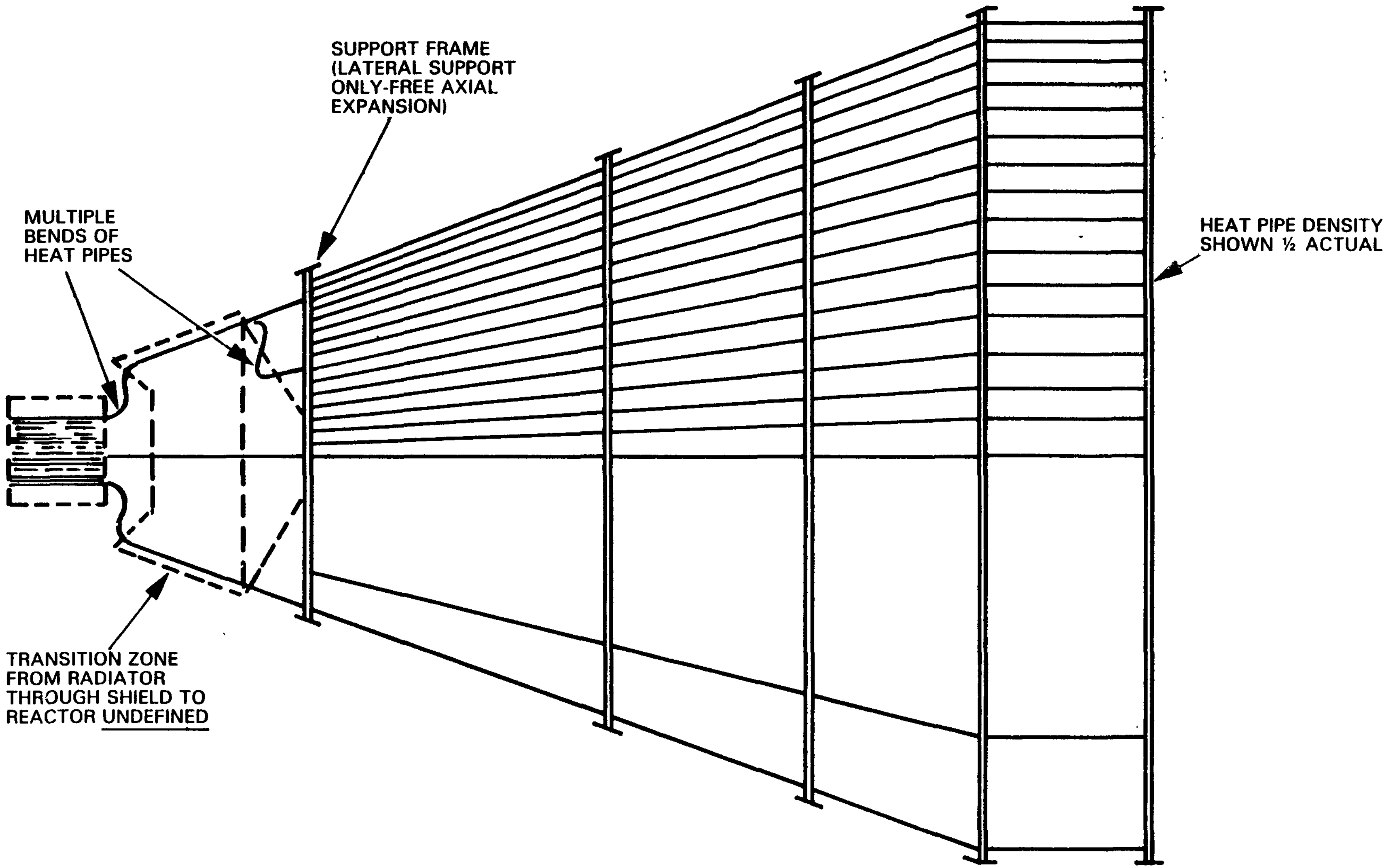

Figure 3.3 Heat Pipe Support & Routing

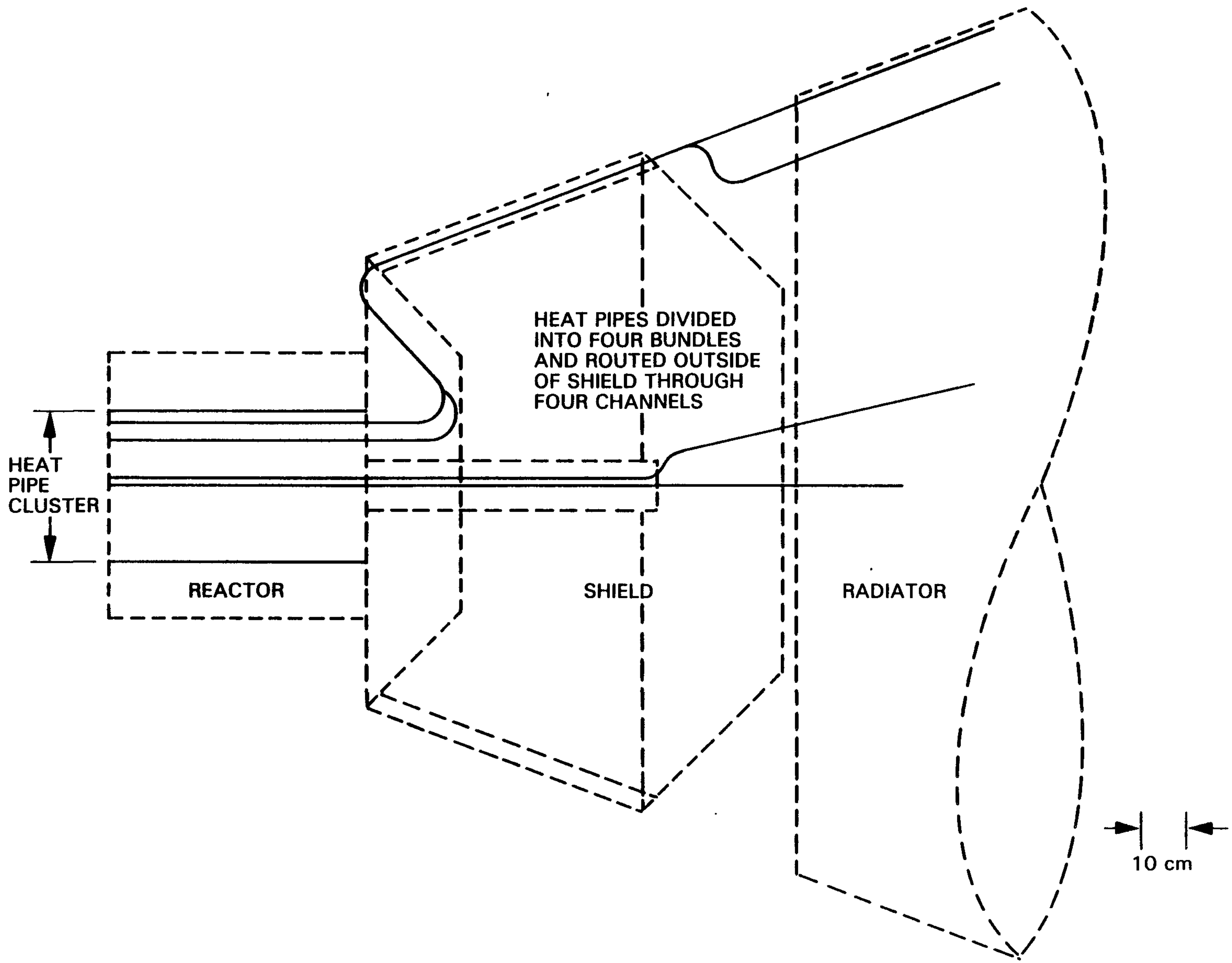

Figure 3.4 Multiple Bend Routing of Heat Pipes Around Shield

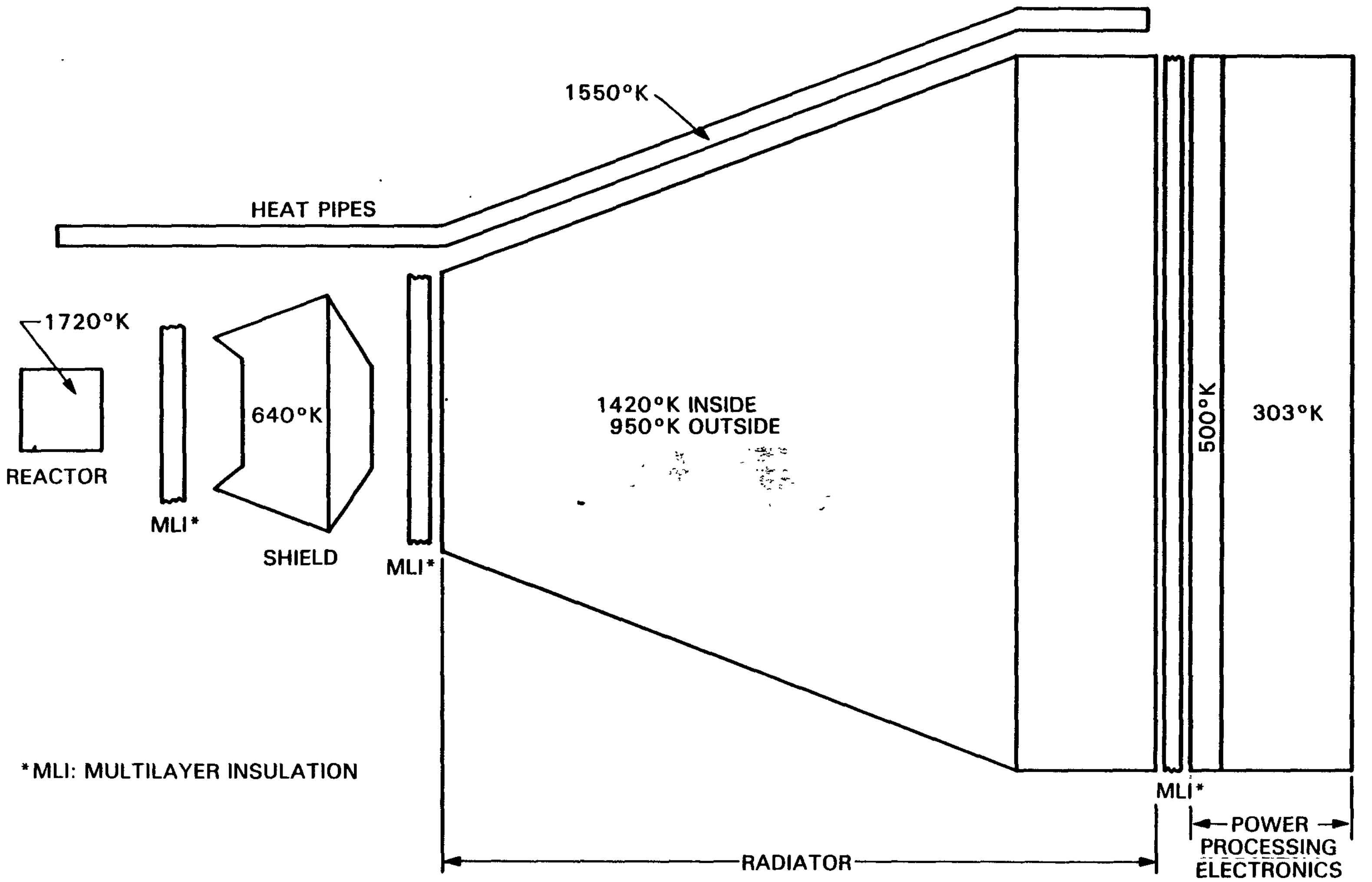

Figure 3.5 Thermal Control Zones

Table 3-2

Assumptions Used In Establishing Preliminary SP-100 Thermal Zones

1. Maximum allowable temperature of the power processor = 320 ^{o}K.
2. Power dissipated is 2000 watts.
3. Copper wire crossections from the TE's to the power processor is 3.2 cm^2.
4. Circular orbit with an altitude of 400 NM.
5. Radiator emittance is 0.75 with a solar absorbtance of 0.15.
6. Support of the power processor radiator section is by 6 titanium tubes, 0.3 meters long, 2.5 cm in diameter with a wall thickness of 0.15 cm.
7. The power processing radiator length is 1 meter.
8. The TE radiator temperature is 950 ^{o}K.
9. The cable radiator length is 0.25 meters.
10. The unsupported cable length between both the TE radiator and the cable and electronics radiators are one foot.

the temperatures of the evaporator and condenser, start-up time, the presence of noncondensable gases, the amount of working fluid and the dormant conditions. Since the heat pipe configuration is new (length, diameter, multiple bends, fluid and container material, wick characteristics), considerable analysis and life testing is strongly recommended to prove out the concept.

The reactor thermal control zone, by virtue of its elevated temperature, presents a set of unique problems which center around control and materials compatibility. The reference reactor design uses control drums and actuators to regulate reactor thermal output. The effects of elevated temperature and radiation on the actuators, bearings, etc., will require more analysis. The reaction of the heat pipe material (Mo-Re) with the reactor fuel elements (UO_2) in this environment is unknown. In addition, it would be desirable to thermally shield the reactor from space to conserve heat and reduce the reactor size. However, the effects of using multilayer insulation in a high nuclear radiation environment are not known and must be determined. Since it is not feasible to test these components in this service environment for the lifetime of the reactor system, a very comprehensive materials accelerated test program is recommended as a high priority consideration.

The radiation shield thermal control zone presents the designer with a difficult challenge. The overriding consideration is the desire to maintain the shield between 600^{o}K (the lower limit to allow reabsorbtion of radioalitically decomposed hydrogen) and 675^{o}K (the upper limit to avoid hydrogen loss due to thermal dissociation if the LiH container(s) is punctured by meteoroids). A simplified, geometrically conceptual configuration is shown in Figure 3.6. The concept shown is oversimplified because it may not be possible to thermally control the shield in the passive manner indicated. Combined thermal/radiation analysis has shown that the shield temperature is very sensitive to the gamma and neutron heating rates into the tungsten (W) and lithium hyride (LiH), respectively, and to the tungsten thickness.

The technique used to integrate the shielding, structural, and thermal control requirements will greatly influence the shield design. Maintaining the LiH at a controlled temperature requires transferring heat from its interior to its outer surfaces. The thermal conductance of LiH is poor so it must be enhanced. It's possible that the structural components of the shield material can be designed to improve thermal control by providing extra conduction paths to the exterior radiating surface of the shield. Otherwise, it appears that active cooling, i.e., pumped loops, may be required.

Another possible approach/trade is to re-evaluate meteoroid puncture probability since that is the major determinant of the 675^{o}K limit. Enhanced meteoroid shielding in the form of radiators on the surface of the shield (like louvers) could significantly lower the probability of puncture.

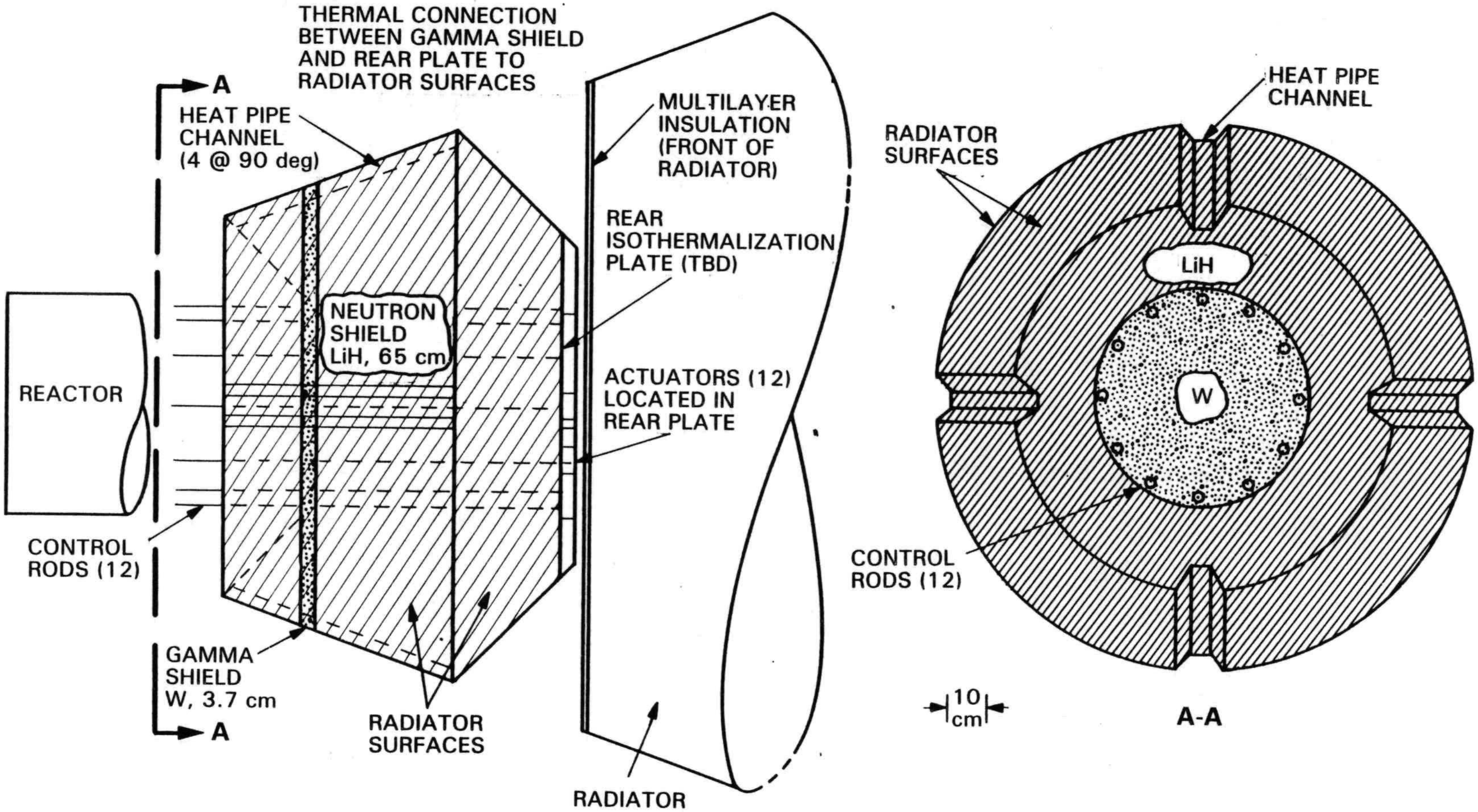

Figure 3.6 Conceptual Radiation Shield Configuration

The thermoelectric conversion/radiator thermal control zone presents special problems because of its dual nature. The interior, with its thermoelectric elements is estimated at $1420^{o}K$. The exterior, which radiates away waste heat, is estimated at $950^{o}K$. In addition, axial thermal gradients of unknown magnitude will occur due to start-up and shut down transients. When solar heating and eclipse (Earth's shadow) transients are added to this large, shell-type structure, the potential for significant stresses and deformation is apparent.

Another issue that will require resolution is the maintenance of the long term surface properties of the radiator. There is currently no known surface finish that will provide a high thermal emittance at $950^{o}K$ for a multiyear lifetime.

The concept of a power processor radiator thermal control design is driven by the requirement that power processor electronics must by kept below $320^{o}K$. The conceptual configuration to satisfy the above temperature requirements is shown presented in Figure 3.5. The concept is based on the assumptions listed in Table 3.2. The power processor electronics are attached to the inside of a cylindrical radiator which is a geometrical extension of the TE radiator. This extended radiator section is thermally isolated from the TE radiator by the use of titanium tube supports and Multilayer Insulation (MLI). The radiator must be of sufficient size to reject the power dissipated by the power processor electronics, the heat flows through the mechanical supports, the heat flows through the MLI, the heat from the copper electrical cables and the heat absorbed from the orbital environment.

The radiator is mechanically supported by 6 titanium tubes that are each 2.5 meters long, 5.0 cm in diameter with a wall thickness of .15 cm. Titanium is used because of its high strength, its tolerance to high temperatures and its low thermal conductance. There are MLI blankets on the aft end of the TE radiator and on the inside surface of the extended radiator to minimize the heat radiated from the TE radiator to the extended radiator. The copper electrical cables that exit the TE radiator section are first thermally attached to the cable radiator to reduce their temperature (and the heat to the extended radiator) before they are attached to the power processor electronics.

3.3 Mass Estimate

The masses of the various SP-100 subsystems are compiled in Table 3.3. As an aid in gauging the range and credibility of the masses, estimates from three sources are included: (1) the original SP-100 design (Reference 1), (2) the reference concept based on a 20° cone (the basis of this report), and (3) the final report from the Nuclear Electric Propulsion (NEPS) study (Ref. 3).

The updated reactor mass estimate is based on a revision of the original SP-100 work. No conceptual design work was performed on this subsystem during this phase of the effort: the estimate is based on information provided in Ref. 2.

The radiation shield mass estimate is felt to be the greatest uncertainty. The 1360 Kg estimate shown is probably conservative since the shield geometry mass is based on simple planar sections (Figure 3.6) with no allowance made for the potential of integrating the structure and other components into the shielding function which could provide significant attenuation of the gamma radiation. A recommended area for future study is the integration of the other subsystems into the radiation shield requirements as suggested in Ref. 4.

The mass estimate with the greatest credibility is the thermoelectric radiator which was derived from Section 4.1. A multi-point shuttle interface was assumed through cradles located to minimize structural loading. Because of the shell nature of the radiator which makes it susceptible to failure by buckling, Beryllium panels were sized as opposed to the carbon/carbon used in the original design (with an attendant 2:1 weight advantage). Attention is called to the fact that the radiator panels were sized with their own integral support framework in the form of raised flanges on all four edges.

The distribution of these estimated subsystem masses location is shown in Table 3.4 in a format different from Table 3.3. That is, distributed among four basic subsystems: reactor, shield, conversion, and radiator. This was done so that the SP-100 thermoelectric reference design could be compared to other systems using different conversion cycles that resolve into these same basic subsystems and parameters such as specific mass and specific prime radiator area.

Table 3.3 Compilation Of SP-100 Mass Estimates (Kg)

	Subsystem	Mass Estimate 1 Original Concept	 2 Reference Design	 3 NEPS	Comment
1.0	REACTOR	453.1	439.9	419.0	2 Updated based on 20 conical radiator, Ref 2
1.1	Fuel and Fin	185.0	---	---	
1.2	HP Mass to Exit	20.0	---	---	
1.3	Inner, Outer Cans, Multifoil	9.0	---	---	
1.4	Fuel Module Support	5.0	---	---	
1.5	Reflector	150.0	---	---	
1.6	Actuators	42.0	---	---	
1.7	Structure	29.0	---	---	
1.8	Reactor Control	10.0	---	---	
1.9	B4C Plug	3.1	---	---	
2.0	RADIATION SHIELD	790.0	1359.89	761.0	2 Probably Conservative
2.1	Attach Truss (Fwd)	---	1.0	---	End Fittings TBD, Ref. 25
2.2	LiH + Container	485.0	496.84	---	
2.3	W	305.0	648.62	---	
2.4	LiH/W Integration	---	---	---	TBD
2.5	Isothermal Plate	---	209.43	---	
2.6	Attach (Aft) + Truss	---	4.0	---	End Fittings TBD, Ref. 25

Table 3.3 Compilation Of SP-100 Mass Estimates (Kg) (C O N T I N U E D)

	Subsystem	Mass Estimate 1 Original Concept	 2 Reference Design	 3 NEPS	Comment
3.0	HEAT PIPES	460.0	272.39	230.0	
3.1	Outside Reactor	460.0	272.39	---	1 Based on 8.7 M Length 2 Based on 5.8 M Length
3.2	Inside Reactor	---	---	---	Incl. in 1.0 Reactor
3.3	Support Frame	---	---	---	Incl. in 6.0
4.0	CONVERSION/RADIATOR	638.0	750.82	576.0	
4.1	Cold Shoe	98.0	133.0	78.0	1 Based on 69.12 M^2, C-C 2 Based on 48.71 M2, Be, Ref. 25
4.2	Hot Shoe	101.2	74.86	60.0	1 Based on 220,000
4.3	T'Couples	138.8	166.21	53.0	2 Based on 168,424
4.4	Multifoil-Radiator	205.0	142.25	220.0	
4.5	Multifoil-End Plate	80.0	85.24	100.0	
4.6	Multifoil-Fwd	5.0	12.56	---	
4.7	Interconnects	10.0	66.70	65.0	2 Ref. 4
4.8	Fwd. Support Ring	---	13.00	---	Be, Ref. 25
4.9	Aft Support Ring	---	57.00	---	Be, Ref. 25

Table 3.3 Compilation Of SP-100 Mass Estimates (Kg) <u>(C O N T I N U E D)</u>

	Subsystem	Mass Estimate 1 Original Concept	 2 Reference Design	 3 NEPS	Comment
5.0	POWER CONDITIONING, CONTROL	130.0	520.5	211.0	
5.1	Computer	10.0	25.0	25.0	NEPS estimates used
5.2	Start-up/Restart (storage)	110.0	120.0	120.0	
5.3	Housekeeping	10.0	36.0	36.0	
5.4	Cabling	---	129.5	---	Ref. 4
5.5	Shunt/Isolation Switches	---	25.0	---	Ref. 4
5.6	Switch Gear	---	TBD	---	Ref. 4
5.7	Contingency	---	50.0	---	Ref. 4
5.8	Cable Radiator	---	29.0	---	Ref. 25
5.9	Equipment Radiator	---	81.0	---	Ref. 25
5.10	Radiator Trusses	---	25.0	---	Ref. 25
6.0	INTEGRATION STRUCTURE, USER INTERFACE	250.0	250.0	470.0	2 Based on original estimate
7.0	AIRBORNE SUPPORT EQUIPMENT	1000.0	1000.0	1990.0	2 Based on original estimate S/C Support incl. in NEPS.
	TOTAL	3721.1	4593.5	4657.0	

Table 3.4

Mass Distribution/Parameters
Of SP-100 Reference Design

Subsystem	Mass (kg)	Fraction of Total	Specific Mass kg/kwe	Specific Prime Radiator Area M /kwe
Reactor	439.9	0.12	5.33	---
Shield	1359.89	0.38	16.46	---
Conversion	1340.71	0.37	16.46	---
- Hot Shoe	74.86			
- T'Couples	166.21			
- Insulation	240.05			
- Interconnects	66.70			
- Heat Pipes	272.39			
- Power Cond, Control	520.5			
Radiator	453.0	0.13	5.48	0.59
- Panels (Be)	133.0			
- Fwd. Support Ring	13.0			
- Aft Support Ring	57.0			
- Integration	250.0			
TOTAL	3593.5	1.00	43.5	

Section 4

Discipline Support Summaries

4.1 Preliminary Structural Design

Figure 4.1 shows the preliminary structural design of the SP-100 space powerplant. The following paragraphs set forth the assumptions, design considerations, and a brief description of this preliminary structural design. A structural weight estimate is included, as are recommendations for future work.

Shuttle Interface: Support and Loading

The structural interface between the SP-100 and the shuttle will be through two cradles located to minimize structural loading of the SP-100. These cradles provide non-redundant support at the SP-100 interface so that deformations of the shuttle are not transmitted to the SP-100. Likewise, the cradles transmit the SP-100 loads to the shuttle in a way to provide reactions in permissible directions at the sills and keel of the shuttle. It is assumed the shuttle will accommodate the loads induced. The payload, independently supported in the mid portion of the shuttle bay, may be structurally isolated from the SP-100 by the flexibility of the stowed erectable boom which connects the SP-100 and payload after separation from the shuttle. For these reasons, the structure of the SP-100 need only sustain the loads induced by the shuttle launch environment. As a first estimate of these loads, the Revision 1 August 3, 1979 plot of acceleration versus mass has been employed.

Description and Design Considerations

Figure 4.1 shows the preliminary structural design of the SP-100 space power plant. It also shows the location of and loads reacted at the single forward and three aft SP-100 support/cradle interfaces. The single forward support located at the bottom (nearest the shuttle keel) of the forward end of the shield is a ball joint that reacts axial, lateral and vertical loads. The three aft supports are located at a structural ring provided at the knuckle between the conical and cylindrical portions of the TE radiator. Two of these aft supports are located at the sides (i.e., near the shuttle sills) and react vertical loads only. The third aft support is located at the bottom of the aft structural ring and reacts lateral loads only.

The principal functional elements of the SP-100, i.e., reactor, shield, TE radiator, and power processor radiators, necessarily operate at high and significantly different temperatures. These components are connected to one another by titanium trusses consisting of three bipods each. The titanium provides the necessary strength at elevated temperatures and the truss configuration and the low thermal conductivity of the titanium combine to provide the requisite low conductive heat transfer from component to component. These trusses are all designed against launch-induced loads and are Euler buckling critical.

The TE radiator cold shoe is a frustrum of a conical shell which serves the dual functions of providing the cold junction of the TEs and the major

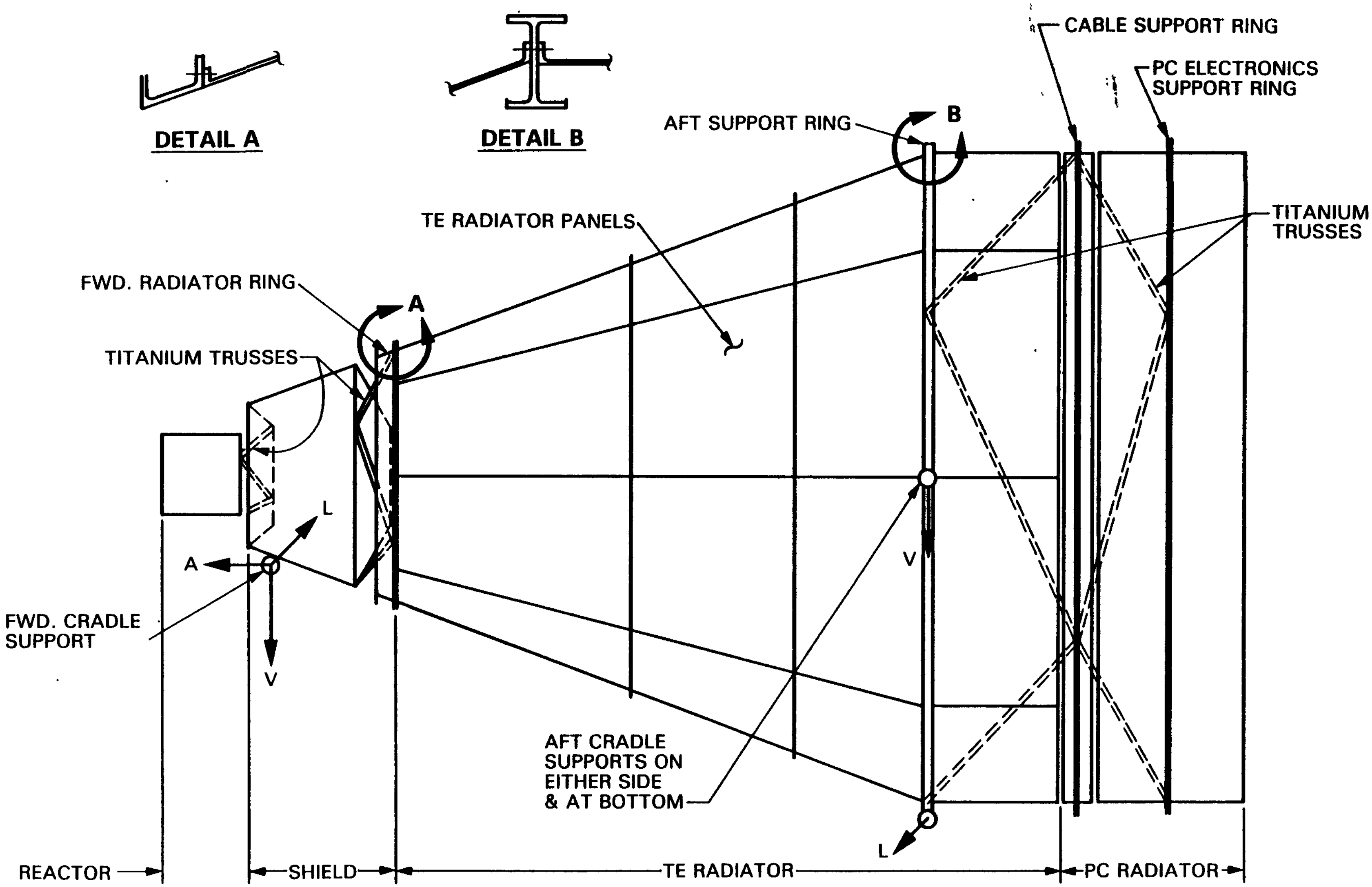

Figure 4.1 Preliminary Structural Design

structural element between the forward and aft supports of the SP-100. This conical shell must sustain the relatively low free-flight maneuver loads while at an operating temperature of approximately $900^{o}K$. At moderate temperatures it must sustain the high launch load environment. This requirement and the thin shell configuration of this component dictate the selection of beryllium as the material of choice due to shell buckling considerations. Carbon/carbon was considered for this component, but its lower Young's modulus/density ratio (quasi-isotropic layup) gives beryllium a weight advantage of nearly two to one. The TE cold shoe consists of 32 equal area beryllium panels which have outward facing flanges on all four sides. These flanges are bolted together to form a complete conical shell.

The aft support ring is located between the juncture of the conical and cylindrical portions of the TE cold shoe. It is required to feed the concentrated reactions at the SP-100 supports into the conical shell. It is beryllium ring of I-section and is stress critical.

The power processor radiators required to cool power cables and power processors are thin-shell aluminum cylinders with stiffening rings. Aluminum provides an acceptable strength-to-weight ratio, can sustain the moderate operating temperatures involved, and provides the desired thermal properties. These radiators are designed as structural rings with in-plane loading and are stress critical. The power processor radiators are attached to each other and to the aft structural ring by means of titanium trusses which provide the requisite low thermal conductivity.

The structural design of the reactor and the shield was not considered during this initial effort. It is assumed that the beryllium housing of the reactor will provide adequate structure to sustain the launch loads. Likewise, the stainless steel (or possibly beryllium) container for the LiH shield can be designed to sustain the launch loads.

Structural Weight

Table 4.1 provides the weight of the structural components described above. Unless otherwise noted, these weights do not include fittings or allowances for joints, these items being greatly influenced by detail design. Structural weight attributable to the reactor and shield is also not included.

Recommendations

Recommendations for further structural design work are included below:

1. Consider structural reliability of beryllium in connection with its use on shuttle.

2. Investigate structural design of reactor and shield.

3. Investigate structural design of shuttle interface cradles.

4. Verify shuttle sill and keel load capability.

5. Consider thermal shock loads during start-up.

6. Consider free-flight maneuver loads.

7. Consider flat TE panels to reduce fabrication costs at a probable decrease in power and structural efficiency.

8. Consider cantilevering SP-100 by payload.

9. Review joint design, especially the joints between the beryllium TE radiator panels.

TABLE 4.1

PRELIMINARY STRUCTURAL WEIGHTS

Item	Description	Mat'l	Weight (kg)	Remarks
Reactor/Shield Truss	1.25" O.D. x .04" wall	Titanium	1	no end fitting allowance
Shield/TE Radiator Truss	2" O.D. x .04" wall	Titanium	4	no end fitting allowance
TE/Cable Radiator Truss	2" O.D. x .063" wall	Titanium	16	no end fitting allowance
Cable/PC Radiator Truss	2" x O.D. x .035^{0} wall	Titanium	9	no end fitting allowance
Fwd TE Radiator Ring	4" x 2" x .25"	Beryllium	13	
TE Radiator Panels	.04" thick	Beryllium	133	Includes .2" x 1" flanges on 4 edges of 32 panels
Aft Support Ring	6" x 4" x .25" I	Beryllium	57	
Cable Radiator	.06" thick & including 2" x 1" x 1/8" I ring	Aluminum	29	
PC Radiator	.06" thick & including 3" x 2" x 1/8" I ring	Aluminum	81	

Notes: 1. Structural weights of reactor and shield have not been estimated.

2. Allowances for fittings and attachments have not been included unless otherwise noted.

4.2 Conceptual Thermal Systems Design

Introduction

The SP-100 power system is divided into five thermal zones according to temperature, as shown in Figure 4.2. Table 4.2 presents an estimate of the heat flows between these zones. A discussion of the thermal aspects of each of these zones and their associated thermal problems is presented here.

Reactor

Most of the internal thermal design will be accomplished by the reactor contractor. We are concerned with thermally integrating the reactor into the overall thermal system.

The present conceptual thermal design assumes that the reactor is covered with a high temperature, multilayer insulation (MLI) blanket. Heat transfer to other zones, other than the heat pipes, is minimized by the use of MLI to attenuate the radiation heat transfer and by the use of thin wall titanium tubing for mechanical supports to attenuate the conduction heat transfer. As can be seen from Table 2, the reactor must generate 1,984,622 watts to supply 1,588,100 watts to the power system while the remaining 396,522 watts is lost through the MLI to space.

Heat Pipes

The heat pipes are the critical link in the heat path between the reactor and the power conversion subsystem. There are several technical questions that must be answered before the heat pipes can be confidently included into the SP-100 power system. These are: startup and shut down performance, long term materials compatibility, and fabricability. Attachment of the heat pipes into the SP-100 system must provide for thermal expansion and contraction during start up, shutdown and operation.

Shield

The shield uses LiH as a neutron absorber and tungsten to attenuate the gamma rays. LiH must be maintained within the temperature range of $600^{o}K$ to $675^{o}K$ to perform satisfactorly. As can be seen from Figure 4.2, the shield is adjacent to 3 zones that operate at a much higher temperature than that desired for the LiH of the shield. The temperature control strategy for the shield would be to thermally isolate the shield as much as possible from the warmer zones and to reject the heat flows through the MLI, as well as that heat generated by neutron capture, from the edges of the shield to space. Thermal isolation from radiant heat transfer is provided by MLI blankets and conduction thermal isolation is provided by the use of thin wall titanium tubes for mechanical support.

The proximity of the shield to the hotter zones, the relatively tight temperature limits, the variation of neutron capture cross section with temperature, the low thermal conductance of the LiH and the penetrations through the shield contribute to the complexity of the thermal design and analysis.

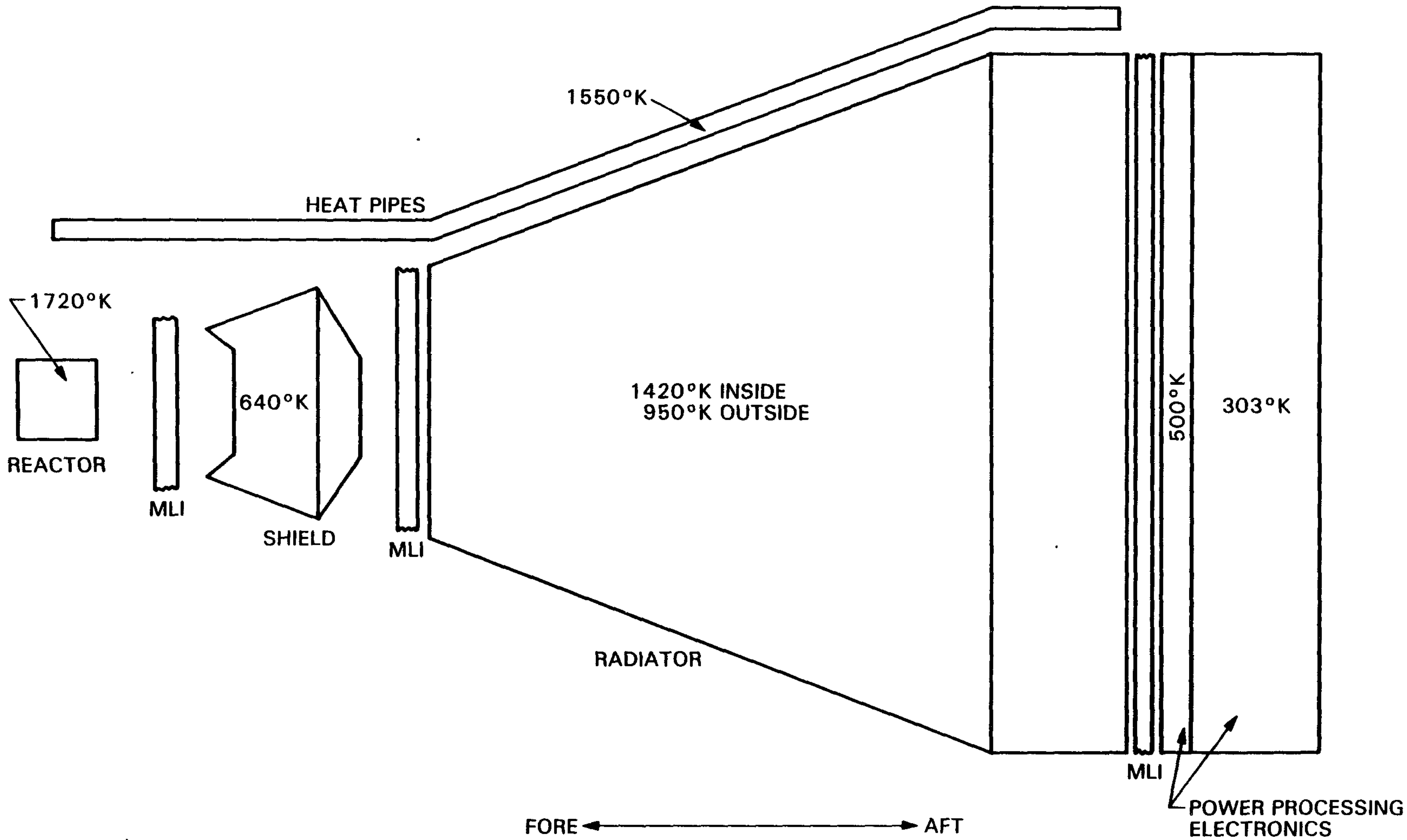

Figure 4.2 Thermal Zones

TABLE 4.2

Preliminary Energy Balance

From \ To	Reactor	Heat Pipes	Shield	Hot Shoe	TE Radiator	Aft Insul	Electronics Radiator	Space
Reactor		1,588,100	482	0	0	0	0	396,522
Heat Pipes			1,085	1,573,710	0	13,305	0	0
Shield				0	0	0	0	1,567
Hot Shoe					1,491,110	0	0	0
TE Radiator						0	7	1,491,110
Aft Insulation							162	16,715
Electronics Radiator								3,492
Space								
Heat Inputs	Int. Gen 1,984,622			Pwr out -82,600		orbital 3,572	orbital 1,330 dissipation 2000	

The conceptual thermal design approach is to use the tungsten to enhance the effective thermal conductance of the LiH to minimize the temperature difference from the center of the shield to its edge. Mechanical louvers would regulate the heat loss to control the bulk temperature. The analysis for the design must be a three dimensional transient model that includes the LiH/titanium composite, the variation of heat generation with temperature and the variation of properties with temperature.

The Radiator

The radiator design as described in Reference 1 appears acceptable at this point in the systems design evolution. The thermoelectric couple spacing combined with the material type and thickness provides a reasonable fin efficiency along the radiator exterior. The insulation between the couples minimize the heat leaks from the hot shoe to the radiator exterior. The high emittance surface finishes of the radiator exterior is the one area that is still not well defined. A MLI blanket is presently attached to the aft end of the radiator assembly to minimize heat loss from the warmer interior and to protect the power pressure electronics zone. This area can also be covered with thermoelectric couples to increase the power to weight ratio.

Electronics

The power processing, control and miscellaneous electronics require a temperature environment of about 20^{o}C. This is provided by a cylindrical section supported from the aft of the radiator zone. The supports are thin wall titanium tubes to minimize the heat conducted from the hot radiator zone. MLI is placed on the inner cylinder surface to minimize the radiation heat transfer from the radiator while the outer surface of this section has a high emittance, low absorbtance surface to radiate its heat to space. A more detailed description of the thermal design, the sizes of the component and the conceptual thermal analysis of the electronics zone is presented in reference 4.

Recommendations

The thermal tasks that must be performed are presented below according to thermal zone.

Reactor

Establish the thermal interfaces with the adjacent zones.

Design and analyze the reactor MLI subsystem.

Shield

Refine the temperature requirements.

Establish the thermal interfaces with the adjacent zones.

Prepare thermal conceptual designs for absolute temperature level control.

Prepare conceptual thermal designs to minimize the internal temperature gradients by using as much as the tungsten as possible.

Prepare analytical models to analyze the above thermal designs.

Determine if the internal heating by neutron capture is significant and if it is a strong function of termperature.

Design the MLI blanket and structural thermal interfaces with the adjacent zones.

Examine the use of active thermal control to meet the stringent temperature requirements.

Heat pipes

Define the heat pipe/SP-100 system interface requirements.

Study the startup/shutdown dynamics for conformance to the interface requirements.

Study the material compatibility of the working fluid, wick structure and container.

Establish if the heat pipes can be fabricated to the SP-100 configuration and still meet the performance requirements.

Radiator

Find a high temperature high emittance outer coating.

Examine the possibility of placing thermoelectric elements on the aft disc section.

Study in more detail the interfaces between the other zones.

Electronics

Define the requirements in more detail.

Establish the thermal interfaces.

Refine the thermal design and analysis as more information becomes available.

SP-100 system

Perform system thermal analysis to determine the thermal interactions between the different zones and the effect of orbital heating on the overall system thermal performance.

4.3 Materials for Primary Radiator Structure

The following materials have been selected as candidates for application to the primary heat rejection subsystem where thermoelectrics are used for energy conversion in the SP-100 system:

- Beryllium, cross-rolled sheet
- Advanced carbon/carbon, two dimensional layups
- Metal matrix composites (Al and Mg matrix)
- Titanium alloys

Initial selection criteria were specific stiffness and specific strength over the temperature range 300^{o} to 950^{o}K.

Typical values for specific stiffness and specific strength of each of the above types of materials are illustrated in Table 4.3 Titanium and its alloys are well characterized with all design data in hand.

Of the three remaining materials, beryllium (Be), carbon/carbon (C/C) composites and metal matrix composites, Be is the best characterized. Development of advanced, 2-dimensional weave C/C composites and of metal matrix composites is still in its infancy.

Since preliminary studies at JPL (see Sect 4.1) have indicated that the primary radiator structural design is dominated by shell buckling considerations, Be, with its high specific stiffness, emerges as the leading candidate material.* Consequently, the following discussion focuses here (see Appendix A) on the mechanical behavior of Be in order to provide a better assessment of its applicability. Future discussion papers will present data on C/C and metal matrix composites.

---

*It's important to note that Be is not the only candidate and that fracture control considerations (including impact resistance) and creep behavior at elevated temperature may drive the selection to one of the other candidate materials.

Table 4.3

PROPERTIES OF METALS USED IN THE AEROSPACE INDUSTRY

Property	Be Sheet	Al 2219-T87	Ti-6A -4V	CRES C455
Density, lb/in^3	0.067	0.102	0.160	0.290
Elastic Modulus, 10^6 psi	42	10.2	16.5	29.0
Ultimate Tensile Strength, 10^3 psi	70	64	150	200
Yield Strength, 10^3 psi	50	50	140	185
Fracture Toughness, ksi $in^{1/2}$	22-27	26	60	85
Specific Strength, 10^5 in	10.4	6.3	9.4	6.9
Specific Stiffness, 10^8 in	6.3	1.0	1.0	1.0

References

(1) JPL Document No. D-389, SP-100 Conceptual Design Description No. 1, June, 1982.

(2) Data Sheet on 20 ^{o} Cone Half Angle Furnished By Richard Ewell, JPL, March, 1983.

(3) Final Report of the Advanced Power and Propulsion Study Phase II - Nuclear Electric Propulsion Implications, K. T. Nock and P. W. Garrison, JPL NO. 725-71, Nov. 1981.

(4) Ideas For Reducing SP-100 Mass, J. W. Winslow, June 13, 1983.

APPENDIX A

Discussion Paper

BERYLLIUM

Beryllium (Be) is toxic as a fine powder, brittle and expensive. Special design, machining and handling techniques are required in production of Be parts. However, Be possesses several unique properties which make it well-suited for spacecraft applications. Its low density and moderate strength and stiffness combine to yield high specific strength (strength/density) and high specific stiffness (modulus/density). The specific strength and stiffness of Be at 25^{o}C are compared with other commonly used aerospace materials in Table I.

The data in Table I demonstrate that, for applications where the design criterion is component tensile strength, titanium and beryllium are the materials of choice. For those cases where high stiffness is desirable, then Be has a 6-fold advantage as indicated by its high specific stiffness compared to Al, Ti and steels.

Tensile Strength

The room temperature tensile strength of hot pressed Be block has been found to range between 45,000 psi and 89,000 psi (2,3). The strength of cross-rolled Be sheet has a guaranteed room temperature ultimate tensile strength (UTS) of of 70,000 psi and yield tensile strength (YTS) of 50,000 psi (10).

The effect of temperature on ultimate tensile strength of Be block and sheet is illustrated in Figure 1. Point 2 shows the range of values from tests (4) where the average value of ultimate tensile strength of hot isostatically pressed (HIP) block was 70,000 psi. The experimental data ranged between 58,000 and 89,000 psi.

Point 3 in Figure 1 also represents data taken on hot pressed Be block (2). The average ultimate tensile strength was 51,000 psi and data ranged between 49,000 and 59,000 psi. Curves 1 and 4-7 represent data taken on cross-rolled Be sheet. The tensile strength drops to approximately one-half the room temperature value at 700^{o} to 800^{o}K. Above 800^{o}K creep of beryllium structures becomes a major consideration.

Work by Odegard (4) demonstrated the dependence of strength on grain size of hot isostatically pressed (HIP) Be. Ultimate strength and yield strength followed the Hall-Petch relationship with highest strengths observed at smallest grain size.

Table 1

PROPERTIES OF METALS USED IN THE AEROSPACE INDUSTRY

Property	Be Sheet	Al 2219-T87	Ti-6A -4V	CRES C455
Density, lb/in^3	0.067	0.102	0.160	0.290
Elastic Modulus, 10^6 psi	42	10.2	16.5	29.0
Ultimate Tensile Strength, 10^3 psi	70	64	150	200
Yield Strength, 10^3 psi	50	50	140	185
Fracture Toughness, ksi $in^{1/2}$	22-27	26	60	85
Specific Strength, 10^5 in	10.4	6.3	9.4	6.9
Specific Stiffness, 10^8 in	6.3	1.0	1.0	1.0

Data from Ref's. 1, 6, & 10.

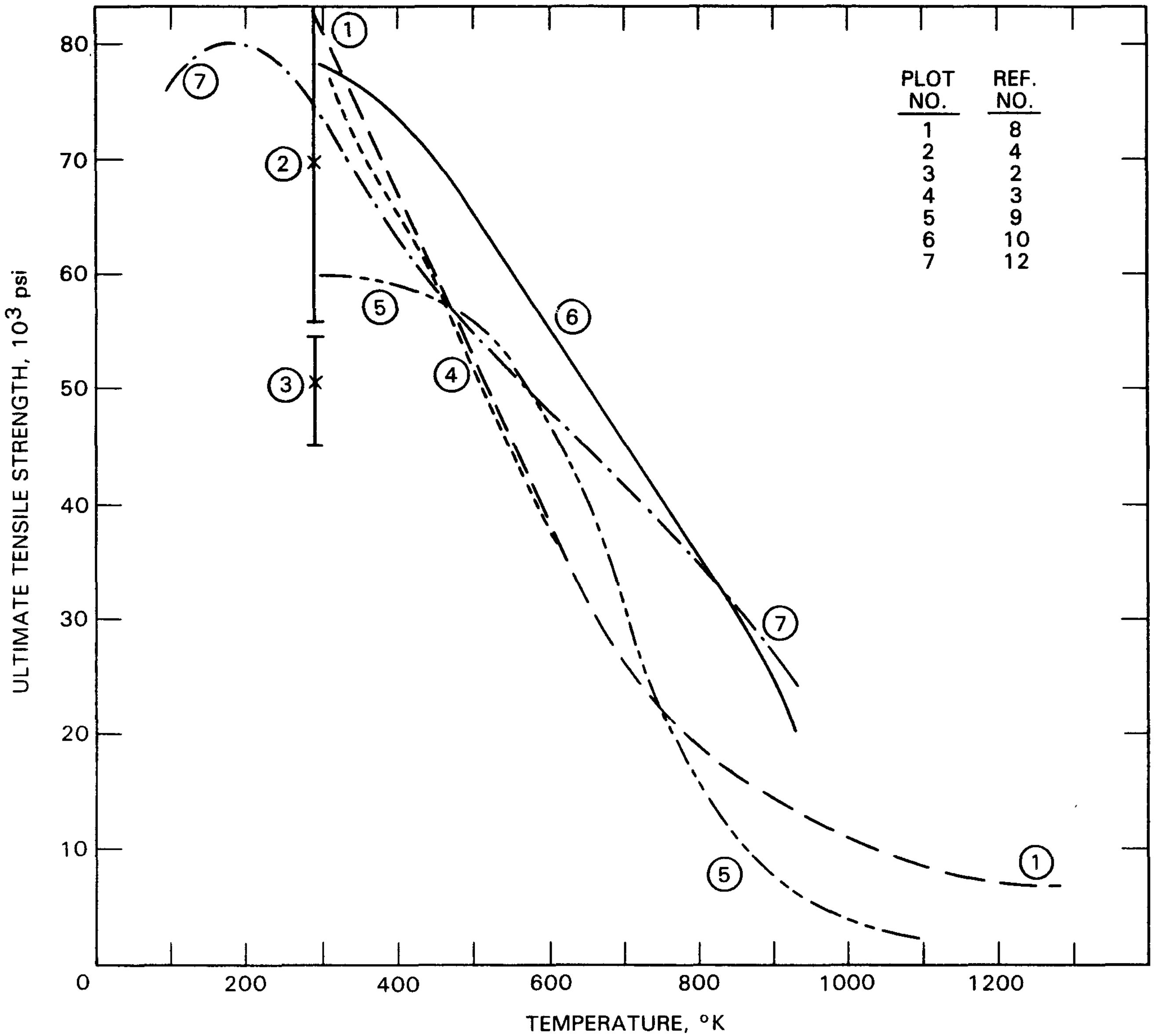

Figure 1 Ultimate Tensile Strength of Beryllium
Block (Points 2 & 3) & Sheet (Curves, 1, 4, 5, 6 & 7)

The best values for ultimate tensile strength of HIP Be were in the 85 to 90 ksi range whereas the lowest values were in the 56 to 60 ksi range. The average value for UTS at room temperature was 70 ksi (specific strength level of 10.4×10^5 in.).

Odegard also found that the ductility was reduced by increase in the BeO oxide content or by decrease in grain size. Strength was found to increase from approximately 14,500 psi as the metallic impurity level increased from approximately 200 ppm to approximately 2000 ppm.

Yield Strength

The effect of temperature on tensile yield strength of cross-rolled sheet and hot pressed block is illustrated in Figure 2. Curves 1 and 2 represent data on cross-rolled SR200 sheet and Point 3 is the minimum room temperature value guaranteed by Brush/Wellman, Inc. Curve 4 represents data on hot pressed Be block from the Aerospace Structural Materials Handbook (12). This last curve is a composite of two sets of data, both of which agree well with one another. At cryogenic temperatures, the yield strength of Be sheet is approximately 60,000 psi. The yield strength begins to decrease above 300^{o}K, however, and reaches about one half the room temperature value at approximately 800^{o}K. Above 800^{o}K, structural design becomes creep limited.

Young's Modulus

The Young's modulus of Be is generally accepted to lie within the range 42 to 46 X 10^6 psi. It is a strong function of porosity and a weak function of forming method. For example the Young's modulus of hot pressed Be block, -100% dense, is approximately 45.5 X 10^6 psi and decreases to approximately 18 X 10^6 psi when 75% of theoretical density (7).

The effect of temperature on the modulus of cross-rolled Be sheet is illustrated in Figure 3. Curves 1 and 2 were determined by an ultrasonic method on two types of cross-rolled sheet. The method of measurement of Young's modulus for Curve 3 was not specified. It may well be that Curve 3 was determined from the slope of stress-strain curves obtained at different temperatures.

Creep

Be creeps at a rapid rate above 800^{o}K (18). The time to produce 0.5% plastic creep in cross-rolled Be sheet as a function of temperature is illustrated by the dotted lines in Figure 4. The material was made from Brush Wellman Inc. Grade S200-E containing approximately 2% BeO (10).

Creep is a function of impurity level. Figure 5 illustrates the effect of purity on creep rate of hot isostatically pressed Be (18).

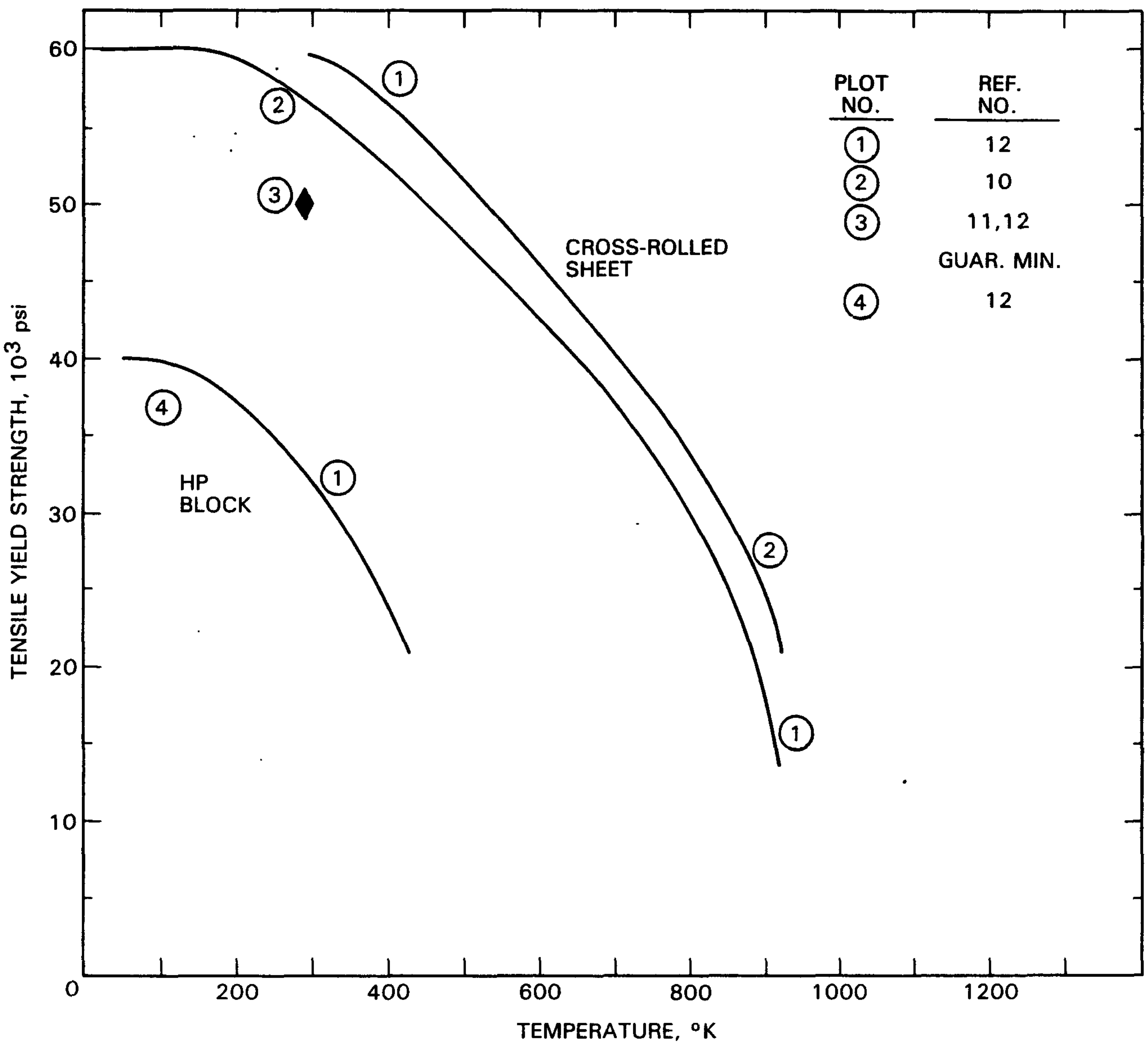

Figure 2 Tinsile Yield Strength of Be Block & Sheet

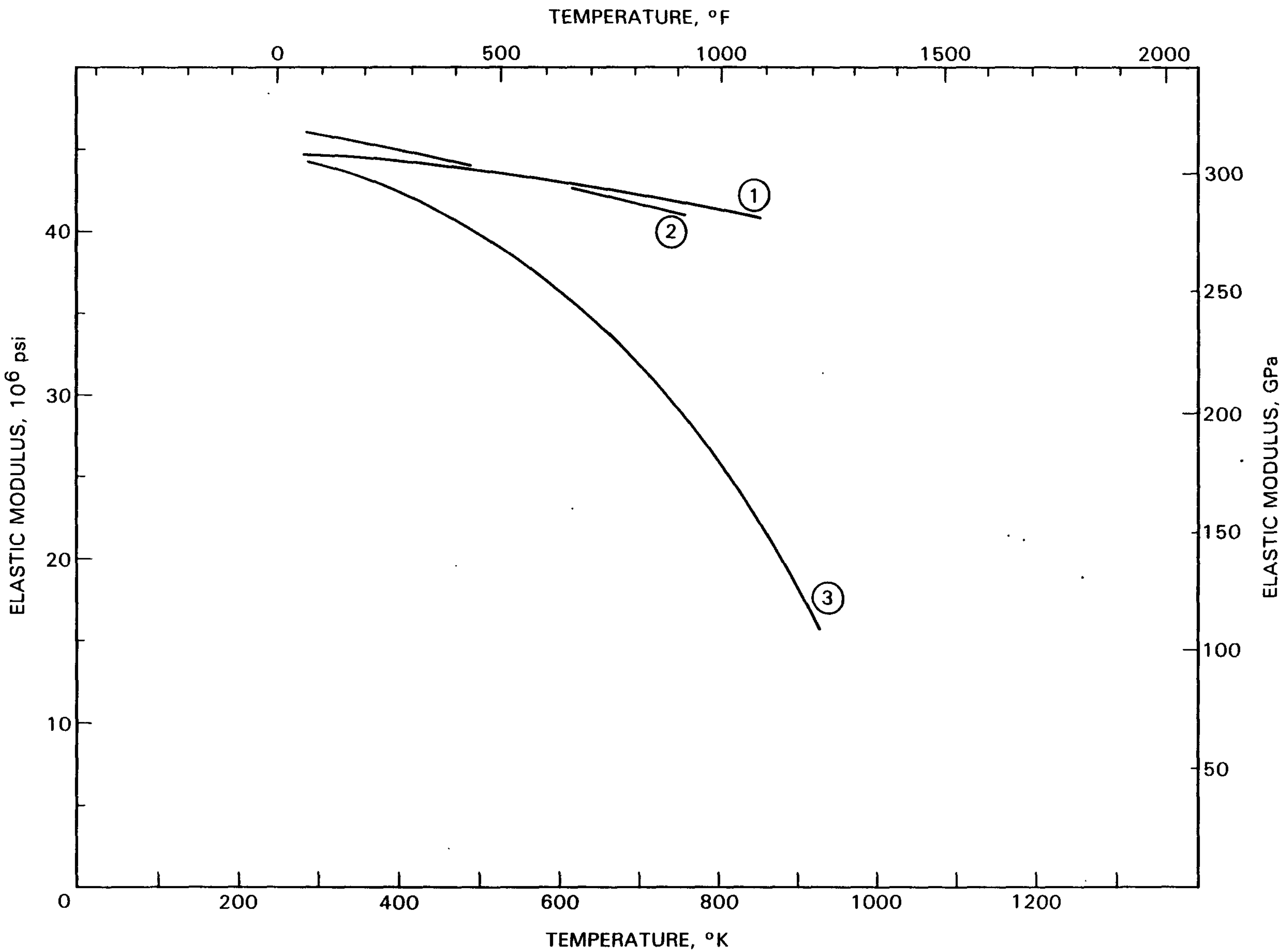

Fig 3. Elastic Modulus of Be
Cross-Rolled Sheet

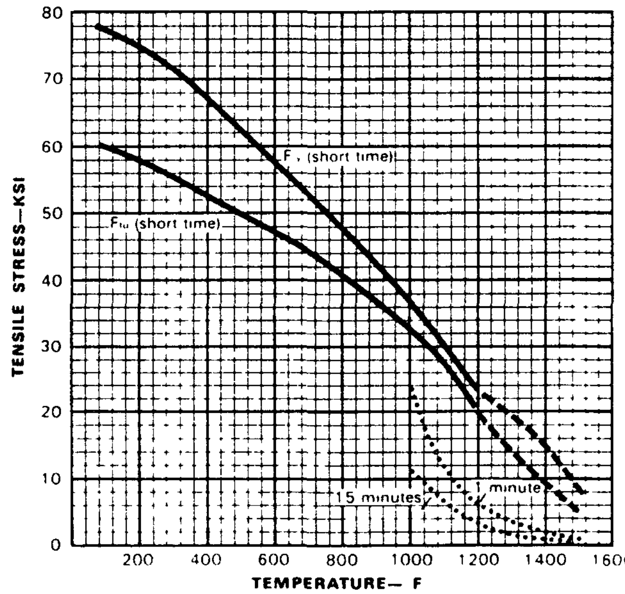

Figure 4. Creep Stress and Time to Produce 0.5% Plastic Creep in Cross-Rolled Beryllium Sheet (from Ref. 10).

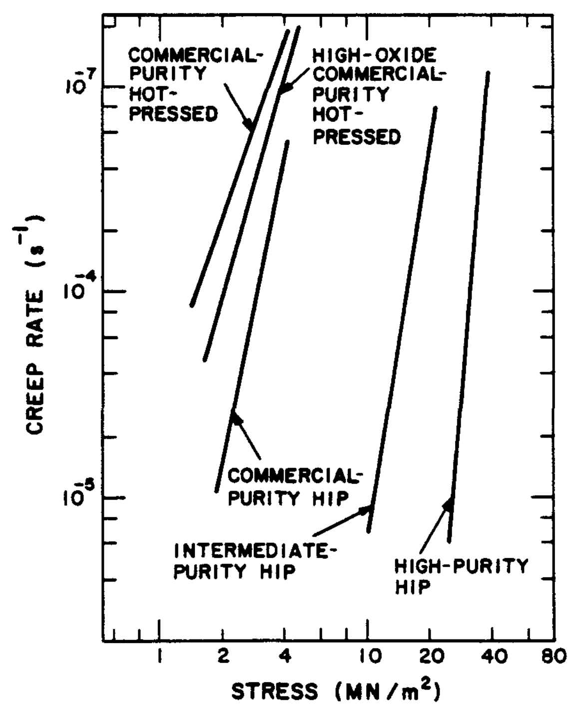

Figure 5. Steady State Creep Data at 1255°K for Several Powder Product Beryllium Materials (from Ref. 18).

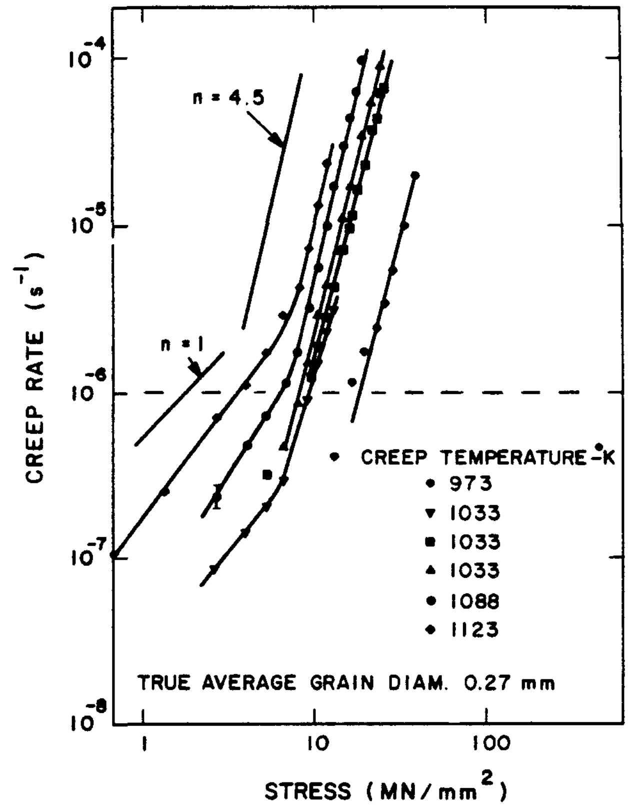

Figure 6. Summarized Creep Data for High Purity Beryllium at Constant Grain Size (from Ref. 18).

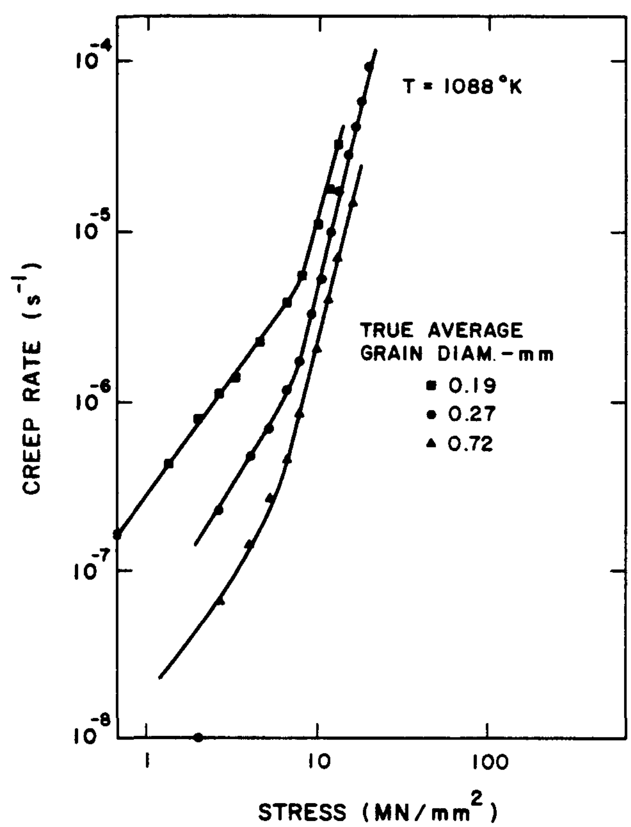

Figure 7. Summarized Creep Data for High Purity Beryllium at Constant Temperature (from Ref. 18).

The role of temperature on creep rate of high purity Be with an average grain size of 0.27 mm is shown in Figure 6 (18). Note that a steady-state creep rate of 10^{-6} sec^{-1} will yield a 0.5% creep strain in 1.4 hour and, at 10^{-8} sec^{-1} 0.5% creep strain is achieved in 139 hours. This demonstrates the need for long-term tests since creep data is generally not extrapolated more than an order of magnitude in time with any, degree of confidence.

The creep rate can be reduced by increasing grain size as illustrated in Figure 7. (18). However, increasing grain size lowers the ultimate tensile strength and tensile yield strength. It is thus necessary to have a knowledge of the anticipated service loads in order to design the material for optimum performance. It should be noted, however, that on the basis of specific creep strength, high purity Be will allow a lighter structure than TD nickel for service up to 1350^{o}K (18).

Fracture Toughness

The mode one, critical stress intensity factor (fracture toughness) of HIP Be was found to range between 8 and 16 ksi/ in and was highest for the highest purity Be (4). Grain size appeared to have no effect on toughness. The role of BeO on toughness could not be ascertained.

Fracture toughness of cross-rolled Be sheet ranged between 28 and 32 ksi/ in for 0.020 in thick sheet and between 22 and 27 ksi/ in for 0.035 in thick sheet (6).

The variation in fracture behavior of ten hot pressed blocks made from S200E powder and S65 powder representing circa 1982 production was studied. It was found that there was a significant difference in K_{IC} in test specimens with cracks oriented normal to the pressing direction (8.96 ksi/ in ±0.33 ksi/ in) compared with specimens with cracks oriented parallel to the pressing direction (10.05 ksi/ in ±0.74 ksi/ in).

Data on fatigue crack growth rates in one specimen from a hot pressed S200E Be block and two specimens from the hot pressed S65 block indicate a threshold stress intensity factor, K_{TH} of between 7.5 and 8.0 ksi/ in. K_{TH} is the applied plane strain stress intensity factor below which crack growth does not occur.

While the data on fracture behavior of hot pressed block is extremely limited (2,6), data on cross-rolled Be sheet is practically non-existant. However, one study in the literature available to me indicated that the fracture toughness of cross-rolled Be sheet ranged between 28 and 32 ksi/ in for 0.020 in. thick sheet and between 22 and 27 ksi/ in. for 0.035 in. thick sheet (6).

Elongation

The elongation to failure at room temperature of cross-rolled Be sheet is a minimum of 10% (10,11). The effect of temperature on elongation to failure is illustrated in Figure 8.

The elongation to failure of hot pressed Be block has been determined to be approximately 1.5% parallel to the pressing direction and approximately 3.0% in the transverse direction (2). Such behavior results from the preferred orientation of the anisotropic Be crystals established during the hot pressing operation.

Ductile-Brittle Transition Temperature

The ductile-brittle transition temperature for Be occurs between 423^{o} and 473^{o}K and can be lowered by increasing purity (3). No additional data are available.

Summary

The ultimate tensile strength and tensile yield strength of cross-rolled Be sheet at room temperature is approximately the same as aluminum and approximately one half that of titanium. However, since the density of Be is approximately 66% that of Al and 42% that of Ti, the mass of Be sheet required to support a specified load is much less than that for Al and slightly less than that for Ti. For example, to support a 1000 lb, axial load with a cylindrical beam, the following mass per unit beam lengths would be required. (It is assumed that the stress is 80% of the UTS and data in Table I are utilized.)

Material	Be	Ti	Al
lb/in.	0.0012	0.00133	0.0020
column dia., in.	0.151	0.103	0.158

Note that while the beam diameter for Be is greater than that for Ti, the mass of the Be beam is approximately 10% less than that of Ti. Mass reduction is of great concern in spacecraft design.

The same type of argument applies when the primary loads on a structural element are buckling loads except that the specific stiffness of a material is used as the figure of merit rather than specific strength. From room temperature to above 800^{o}K, the specific stiffness of Be sheet is greater than that of 2-D C/C composites, Ti alloy and steels.

The creep behavior of Be is not well characterized. What little data is available was performed in air at temperatures above 800^{o}K. No data has been found for creep rates under high stress in the temperature range 400^{o}K to 800^{o}K in vacuum. Since creep mechanisms vary with temperature and

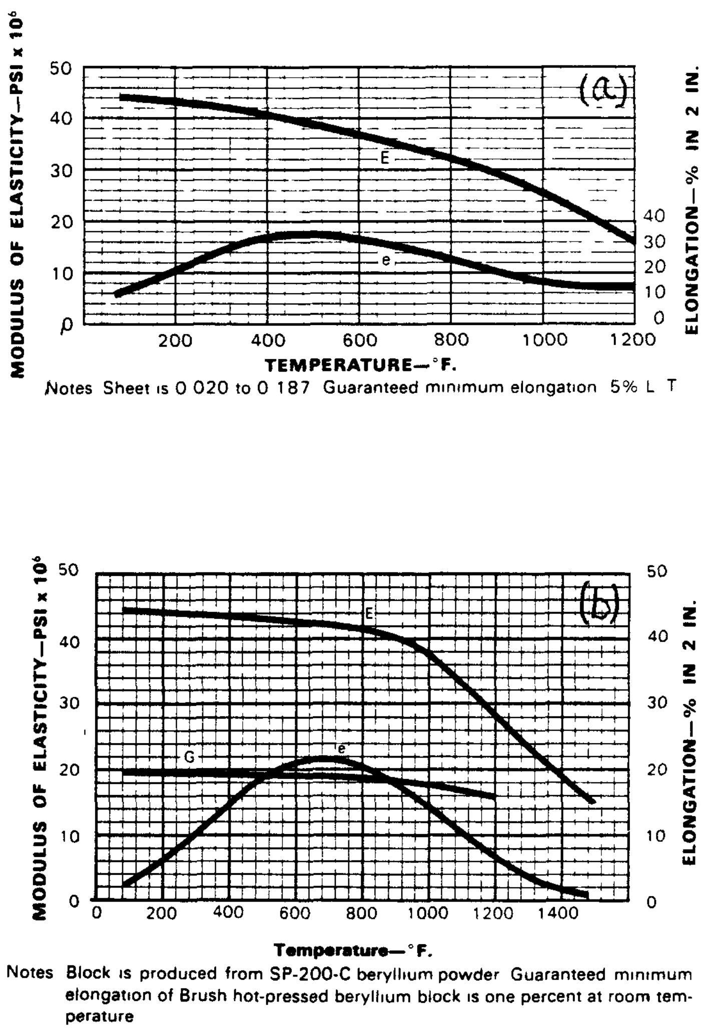

Figure 8. Typical Modulus and Elongation of (a) Cross-Rolled Beryllium Sheet and (b) Hot-Pressed Beryllium Block (from Ref. 10).

stress, creep data cannot be extrapolated with confidence across wide ranges of temperature and stress. Detailed long-term creep studies on current forms of Be are necessary in order to provide sufficient information to the spacecraft designer to instill a degree of confidence in the design.

The fracture toughness and crack growth rates of Be block and sheet need to be understood in greater detail. The effects of grain size, impurity level, temperature and structural anisotropy on fracture control parameters need to be determined in order to (a) provide design information and (b) provide material qualification criteria (i.e., accept/reject criteria).

Additional work is required to better understand the effect of grain size, impurity content, and degree of anisotrophy on the ductile-brittle transition temperature of Be. The effect of strain rate on the DBTT needs to be accounted for.

This review of Be properties has omitted the Be alloys from consideration. It has been suggested (16) that Be with several percent Cu addition may have significantly improved properties. A review of this area is underway.

In addition to being able to withstand the mechanical and thermal loads imposed during launch, boost to user orbit and operation, the structure must have some resistance to hostile threats. While data has been obtained to illustrate the behavior of candidate materials in a laser threat environment (17), no systematic analysis has been performed. However, as the type and level of threat is better defined the requirements will be factored into this assessment.

References for Appendix A

1. R. K. Case, et al., "Beryllium Utilization in Large Spacecraft Mechanisms", Paper 83-0866-CP, 24th AIAA SDM Conference, Lake Tahoe, Nevada, May 2-4, 1983.

2. D. D. Lemon and W. F. Brown, Jr., "Fracture Toughness of Hot-Pressed Beryllium," Paper 83-0870-CP, 24th AIAA SDM Conference, Lake Tahoe, Nevada, May 2-4, 1983.

3. F. W. Cooke, et al., "Affect of Purity and Processing Procedure on the Mechanical Properties of Beryllium Sheet," Met. Trans., 2:1297-1305 (1971).

4. B. C. Odegard, Jr., "The Influence of Purity Level on the Mechanical Properties of Hot Isostatically Pressed Beryllium," SAND 79-8232, September 1979.

5. R. R. Corle, et al., "Identification and Resolution of a Defect in High Strength Beryllium," Paper 83-0781, 24th AIAA SDM Conference, Lake Tahoe, Nevada, May 2-4, 1983.

6. L. A. Grant, "Successful Applications of Beryllium Sheet Materials to Satellite Structures," Paper 83-0950-CP, 24th AIAA SDM Conference, Lake Tahoe, Nevada, May 2-4, 1983.

7. M. P. Baldwin, "The Measurement of the Elastic Moduli of Beryllium by an Ultrasonic Resonance Technique," AWRE Report No. 049/70, August 1970.

8. I. I. Papirov and G. F. Tikhinsky, "Structure and Mechanical Properties of Fine-Grain Formed Beryllium," FTD-HT-23-888-70, January 1971.

9. G. I. Turner and E. G. King, "Tensile Properties of Hot Pressed Beryllium: The Effect of Strain Rate on Properties up to 1100^{o}K," AWRE Report No. 05/72, January 1982.

10. "Designing with Beryllium," Brush Wellman Pamphlet on Beryllium, no date.

11. William Becker, Brush Wellman Co., Personal Communication, July 1979.

12. W. F. Brown, Jr. and B. King, "Be," Aerospace Structural Metals Handbook, Revised June 1974, Code 5105, p. 14.

13. M. H. Jones, et al., "Crack Toughness Evaluation of Hot Pressed and Forged Beryllium," J. of Testing and Eval., ASTM, March 1973, p. 100.

References for Appendix A (Continued)

14. W. O. Shabbits and W. A. Logsdon, "S200 Grade Beryllium Fracture Toughness Properties," ibid., p. 110.

15. H. Conrad, et al., "A Joint Fracture Toughness Evaluation of Hot Pressed Beryllium," 4th International Conference on Beryllium, Paper No. 21, The Metals Society, London, 1977.

16. W. C. Riley, Research Opportunities, Inc., Personal communication, July 1983.

17. R. H. Smoak, Handout entitled "Energy Required for Heating Selected Materials" provided to T. Jordon, J. R. French and the Systems Definition Team illustrating amount of energy required to melt/votatilize selected structural materials, dated 4/21/83.

18. N. R. Borch, "Elevated Temperature Behavior" pp 307-30 in Beryllium Science and Technology, Vol. 1, ed by D. Webster and G. J. London, Plenum Press, New York 1979.

Acknowledgement

The authors gratefully acknowledge the help they received during the course of this study from R. C. Ewell for his consultation on system studies previously performed.

SP-100 Program Distribution List

SP-100 PROGRAM OFFICE

LCDR William E. Wright. Director	DARPA
Delbert F. Bunch. Deputy Director for Nuclear Technology	DOE HQ
Judith H. Ambrus. Deputy Director for Aerospace Technology	NASA HQ

SP-100 PROJECT OFFICE

Vincent C. Truscello, Project Manager	JPL
Herbert S. Davis. Assistant Manager	JPL
John E. Hanson. Deputy Manager for Nuclear Technology	Los Alamos
Jack F. Mondt. Deputy Manager for Aerospace Technology	JPL
James R. French. System Definition Manager	JPL
Richard A. Wallace. Mission Analysis and Requirements Manager	JPL
Kirk G. Gerbracht. Adminstration and Operations Manager	JPL
R. Joseph Sovie. Manager. SP-100 Office	LeRC

PROJECT REVIEW BOARD

SAFETY ADVISORY COMMITTEE

AIR FORCE

Len Caveny	Bolling AFB
Capt. Judith Cook	Kirtland AFB
Lt. Jason Feig	AF/RPL
Lt. Efren Fornoles	Kirtland AFB
Lt. Steven Hoeser	Space Division
Lt. Col. James Lee	Kirtland AFB
Capt. David Perkins	AF/RPL
Jim Reams	Wright-Patterson AFB
Col. Frank J. Redd	Kirtland AFB

ARGONNE NATIONAL LABORATORY

Richard Lewis

BROOKHAVEN NATIONAL LABORATORY

Herb Kouts

DEPARTMENT OF ENERGY

Dyer Kenney	DOE/HQ
Ehsan Khan	DOE/HQ
Stephen Lanes	DOE/HQ
Lt. Col. Robert Smith	DOE/HQ
Walter Von Flue	DOE/SAN

HEDL

C. M. Cox

INEL

John A. Dearien

SP-100 Program Distribution List (Continued)

JOHNSON SPACE CENTER

Will Ellis
J. Gary Rankin

JPL

Internal Distribution

LANGLEY RESEARCH CENTER

Ray Hook

LAWRENCE LIVERMORE NATIONAL LABORATORY

Carl Walter

LEWIS RESEARCH CENTER

Henry Slone
Ronald Thomas

LOS ALAMOS NATIONAL LABORATORY

Jay Boudreau
Kaye D. Lathrop

NASA

Wayne Hudson	Resident Office, Kirtland AFB
Jerome P. Mullin	Headquarters
Frederick Bowen Jr.	Resident Office, JPL

NAVY

Cdr. Larry Burgess	NAVELEX
LCDR William Mohr	NAVELEX
Bill Schmidt	Office of Naval Research
Jim Severance	Naval Research Laboratory

OAK RIDGE NATIONAL LABORATORY

William Harms

SANDIA NATIONAL LABORATORY

Lou Cropp